

A search for the exotic meson $X(5568)$ with the Collider Detector at Fermilab

T. Aaltonen,²¹ S. Amerio^{ll,39} D. Amidei,³¹ A. Anastassov^{w,15} A. Annovi,¹⁷ J. Antos,¹² G. Apollinari,¹⁵
J.A. Appel,¹⁵ T. Arisawa,⁵¹ A. Artikov,¹³ J. Asaadi,⁴⁷ W. Ashmanskas,¹⁵ B. Auerbach,² A. Aurisano,⁴⁷ F. Azfar,³⁸
W. Badgett,¹⁵ T. Bae,²⁵ A. Barbaro-Galtieri,²⁶ V.E. Barnes,⁴³ B.A. Barnett,²³ P. Barria^{nn,41} P. Bartos,¹²
M. Baucé^{ll,39} F. Bedeschi,⁴¹ S. Behari,¹⁵ G. Bellettini^{mm,41} J. Bellinger,⁵³ D. Benjamin,¹⁴ A. Beretvas,¹⁵
A. Bhatti,⁴⁵ K.R. Bland,⁵ B. Blumenfeld,²³ A. Bocci,¹⁴ A. Bodek,⁴⁴ D. Bortoletto,⁴³ J. Boudreau,⁴² A. Boveia,¹¹
L. Brigliadori^{kk,6} C. Bromberg,³² E. Brucken,²¹ J. Budagov,¹³ H.S. Budd,⁴⁴ K. Burkett,¹⁵ G. Busetto^{ll,39}
P. Bussey,¹⁹ P. Butti^{mm,41} A. Buzatu,¹⁹ A. Calamba,¹⁰ S. Camarda,⁴ M. Campanelli,²⁸ F. Canelli^{ee,11} B. Carls,²²
D. Carlsmith,⁵³ R. Carosi,⁴¹ S. Carrillo^{l,16} B. Casal^{j,9} M. Casarsa,⁴⁸ A. Castro^{kk,6} P. Catastini,²⁰ D. Cauz^{ssst,48}
V. Cavaliere,²² A. Cerri^{e,26} L. Cerrito^{r,28} Y.C. Chen,¹ M. Chertok,⁷ G. Chiarelli,⁴¹ G. Chlachidze,¹⁵ K. Cho,²⁵
D. Chokheli,¹³ A. Clark,¹⁸ C. Clarke,⁵² M.E. Convery,¹⁵ J. Conway,⁷ M. Corbo^{z,15} M. Cordelli,¹⁷ C.A. Cox,⁷
D.J. Cox,⁷ M. Cremonesi,⁴¹ D. Cruz,⁴⁷ J. Cuevas^{y,9} R. Culbertson,¹⁵ N. d'Ascenzo^{v,15} M. Datta^{hh,15}
P. de Barbaro,⁴⁴ L. Demortier,⁴⁵ M. Deninno,⁶ M. D'Errico^{ll,39} F. Devoto,²¹ A. Di Canto^{mm,41} B. Di Ruzza^{p,15}
J.R. Dittmann,⁵ S. Donati^{mm,41} M. D'Onofrio,²⁷ M. Dorigo^{uu,48} A. Driutti^{ssst,48} K. Ebina,⁵¹ R. Edgar,³¹
A. Elagin,¹¹ R. Erbacher,⁷ S. Errede,²² B. Esham,²² S. Farrington,³⁸ J.P. Fernández Ramos,²⁹ R. Field,¹⁶
G. Flanagan^{t,15} R. Forrest,⁷ M. Franklin,²⁰ J.C. Freeman,¹⁵ H. Frisch,¹¹ Y. Funakoshi,⁵¹ C. Galloni^{mm,41}
A.F. Garfinkel,⁴³ P. Garosi^{nn,41} H. Gerberich,²² E. Gerchtein,¹⁵ S. Giagu,⁴⁶ V. Giakoumopoulou,³
K. Gibson,⁴² C.M. Ginsburg,¹⁵ N. Giokaris,^{3,*} P. Giromini,¹⁷ V. Glagolev,¹³ D. Glenzinski,¹⁵ M. Gold,³⁴
D. Goldin,⁴⁷ A. Golossanov,¹⁵ G. Gomez,⁹ G. Gomez-Ceballos,³⁰ M. Goncharov,³⁰ O. González López,²⁹
I. Gorelov,³⁴ A.T. Goshaw,¹⁴ K. Goulianos,⁴⁵ E. Gramellini,⁶ C. Grosso-Pilcher,¹¹ J. Guimaraes da Costa,²⁰
S.R. Hahn,¹⁵ J.Y. Han,⁴⁴ F. Happacher,¹⁷ K. Hara,⁴⁹ M. Hare,⁵⁰ R.F. Harr,⁵² T. Harrington-Taber^{m,15}
K. Hatakeyama,⁵ C. Hays,³⁸ J. Heinrich,⁴⁰ M. Herndon,⁵³ A. Hocker,¹⁵ Z. Hong^{w,47} W. Hopkins^{f,15} S. Hou,¹
R.E. Hughes,³⁵ U. Husemann,⁵⁴ M. Hussein^{cc,32} J. Huston,³² G. Introzzi^{ppqq,41} M. Iori^{rr,46} A. Ivanov^{o,7}
E. James,¹⁵ D. Jang,¹⁰ B. Jayatilaka,¹⁵ E.J. Jeon,²⁵ S. Jindariani,¹⁵ M. Jones,⁴³ K.K. Joo,²⁵ S.Y. Jun,¹⁰
T.R. Junk,¹⁵ M. Kambeitz,²⁴ T. Kamon,^{25,47} P.E. Karchin,⁵² A. Kasmi,⁵ Y. Kato^{n,37} W. Ketchum^{ii,11}

J. Keung,⁴⁰ B. Kilminster^{ee},¹⁵ D.H. Kim,²⁵ H.S. Kim^{bb},¹⁵ J.E. Kim,²⁵ M.J. Kim,¹⁷ S.H. Kim,⁴⁹ S.B. Kim,²⁵
 Y.J. Kim,²⁵ Y.K. Kim,¹¹ N. Kimura,⁵¹ M. Kirby,¹⁵ K. Kondo,^{51,*} D.J. Kong,²⁵ J. Konigsberg,¹⁶ A.V. Kotwal,¹⁴
 M. Kreps,²⁴ J. Kroll,⁴⁰ M. Kruse,¹⁴ T. Kuhr,²⁴ M. Kurata,⁴⁹ A.T. Laasanen,⁴³ S. Lammel,¹⁵ M. Lancaster,²⁸
 K. Lannon^x,³⁵ G. Latinoⁿⁿ,⁴¹ H.S. Lee,²⁵ J.S. Lee,²⁵ S. Leo,²² S. Leone,⁴¹ J.D. Lewis,¹⁵ A. Limosani^s,¹⁴
 E. Lipeles,⁴⁰ A. Lister^a,¹⁸ Q. Liu,⁴³ T. Liu,¹⁵ S. Lockwitz,⁵⁴ A. Loginov,⁵⁴ D. Lucchesi^{ll},³⁹ A. Lucà,^{17,15}
 J. Lueck,²⁴ P. Lujan,²⁶ P. Lukens,¹⁵ G. Lungu,⁴⁵ J. Lys,^{26,*} R. Lysak^d,¹² R. Madrak,¹⁵ P. Maestroⁿⁿ,⁴¹
 S. Malik,⁴⁵ G. Manca^b,²⁷ A. Manousakis-Katsikakis,³ L. Marchese^{jj},⁶ F. Margaroli,⁴⁶ P. Marino^{oo},⁴¹ K. Matera,²²
 M.E. Mattson,⁵² A. Mazzacane,¹⁵ P. Mazzanti,⁶ R. McNultyⁱ,²⁷ A. Mehta,²⁷ P. Mehtala,²¹ C. Mesropian,⁴⁵
 T. Miao,¹⁵ D. Mietlicki,³¹ A. Mitra,¹ H. Miyake,⁴⁹ S. Moed,¹⁵ N. Moggi,⁶ C.S. Moon,¹⁵ R. Moore^{ffgg},¹⁵
 M.J. Morello^{oo},⁴¹ A. Mukherjee,¹⁵ Th. Muller,²⁴ P. Murat,¹⁵ M. Mussini^{kk},⁶ J. Nachtman^m,¹⁵ Y. Nagai,⁴⁹
 J. Naganoma,⁵¹ I. Nakano,³⁶ A. Napier,⁵⁰ J. Nett,⁴⁷ T. Nigmanov,⁴² L. Nodulman,² S.Y. Noh,²⁵ O. Norniella,²²
 L. Oakes,³⁸ S.H. Oh,¹⁴ Y.D. Oh,²⁵ T. Okusawa,³⁷ R. Orava,²¹ L. Ortolan,⁴ C. Pagliarone,⁴⁸ E. Palencia^e,⁹
 P. Palni,³⁴ V. Papadimitriou,¹⁵ W. Parker,⁵³ G. Pauletta^{sstt},⁴⁸ M. Paulini,¹⁰ C. Paus,³⁰ T.J. Phillips,¹⁴
 G. Piacentino^q,¹⁵ E. Pianori,⁴⁰ J. Pilot,⁷ K. Pitts,²² C. Plager,⁸ L. Pondrom,⁵³ S. Poprocki^f,¹⁵ K. Potamianos,²⁶
 A. Pranko,²⁶ F. Prokoshin^{aa},¹³ F. Ptohos^g,¹⁷ G. Punzi^{mm},⁴¹ I. Redondo Fernández,²⁹ P. Renton,³⁸
 M. Rescigno,⁴⁶ F. Rimondi,^{6,*} L. Ristori,^{41,15} A. Robson,¹⁹ T. Rodriguez,⁴⁰ S. Rolli^h,⁵⁰ M. Ronzani^{mm},⁴¹
 R. Roser,¹⁵ J.L. Rosner,¹¹ F. Ruffiniⁿⁿ,⁴¹ A. Ruiz,⁹ J. Russ,¹⁰ V. Rusu,¹⁵ W.K. Sakumoto,⁴⁴ Y. Sakurai,⁵¹
 L. Santi^{sstt},⁴⁸ K. Sato,⁴⁹ V. Saveliev^v,¹⁵ A. Savoy-Navarro^z,¹⁵ P. Schlabach,¹⁵ E.E. Schmidt,¹⁵ T. Schwarz,³¹
 L. Scodellaro,⁹ F. Scuri,⁴¹ S. Seidel,³⁴ Y. Seiya,³⁷ A. Semenov,¹³ F. Sforza^{mm},⁴¹ S.Z. Shalhout,⁷ T. Shears,²⁷
 P.F. Shepard,⁴² M. Shimojima^u,⁴⁹ M. Shochet,¹¹ I. Shreyber-Tecker,³³ A. Simonenko,¹³ K. Sliwa,⁵⁰ J.R. Smith,⁷
 F.D. Snider,¹⁵ H. Song,⁴² V. Sorin,⁴ R. St. Denis,^{19,*} M. Stancari,¹⁵ D. Stentz^w,¹⁵ J. Strologas,³⁴ Y. Sudo,⁴⁹
 A. Sukhanov,¹⁵ I. Suslov,¹³ K. Takemasa,⁴⁹ Y. Takeuchi,⁴⁹ J. Tang,¹¹ M. Tecchio,³¹ P.K. Teng,¹ J. Thom^f,¹⁵
 E. Thomson,⁴⁰ V. Thukral,⁴⁷ D. Toback,⁴⁷ S. Tokar,¹² K. Tollefson,³² T. Tomura,⁴⁹ D. Tonelli^e,¹⁵ S. Torre,¹⁷
 D. Torretta,¹⁵ P. Totaro,³⁹ M. Trovato^{oo},⁴¹ F. Ukegawa,⁴⁹ S. Uozumi,²⁵ F. Vázquez^l,¹⁶ G. Velev,¹⁵ C. Vellidis,¹⁵
 C. Vernieri^{oo},⁴¹ M. Vidal,⁴³ R. Vilar,⁹ J. Vizán^{dd},⁹ M. Vogel,³⁴ G. Volpi,¹⁷ P. Wagner,⁴⁰ R. Wallny^j,¹⁵ S.M. Wang,¹

D. Waters,²⁸ W.C. Wester III,¹⁵ D. Whiteson^{c, 40} A.B. Wicklund,² S. Wilbur,⁷ H.H. Williams,⁴⁰ J.S. Wilson,³¹

P. Wilson,¹⁵ B.L. Winer,³⁵ P. Wittich^{f, 15} S. Wolbers,¹⁵ H. Wolfmeister,³⁵ T. Wright,³¹ X. Wu,¹⁸ Z. Wu,⁵

K. Yamamoto,³⁷ D. Yamato,³⁷ T. Yang,¹⁵ U.K. Yang,²⁵ Y.C. Yang,²⁵ W.-M. Yao,²⁶ G.P. Yeh,¹⁵ K. Yi^{m, 15} J. Yoh,¹⁵

K. Yorita,⁵¹ T. Yoshida^{k, 37} G.B. Yu,¹⁴ I. Yu,²⁵ A.M. Zanetti,⁴⁸ Y. Zeng,¹⁴ C. Zhou,¹⁴ and S. Zucchelli^{kk6}

(CDF Collaboration)[†]

¹*Institute of Physics, Academia Sinica, Taipei, Taiwan 11529, Republic of China*

²*Argonne National Laboratory, Argonne, Illinois 60439, USA*

³*University of Athens, 157 71 Athens, Greece*

⁴*Institut de Fisica d'Altes Energies, ICREA, Universitat Autònoma de Barcelona, E-08193, Bellaterra (Barcelona), Spain*

⁵*Baylor University, Waco, Texas 76798, USA*

⁶*Istituto Nazionale di Fisica Nucleare Bologna, ^{kk}University of Bologna, I-40127 Bologna, Italy*

⁷*University of California, Davis, Davis, California 95616, USA*

⁸*University of California, Los Angeles, Los Angeles, California 90024, USA*

⁹*Instituto de Fisica de Cantabria, CSIC-University of Cantabria, 39005 Santander, Spain*

¹⁰*Carnegie Mellon University, Pittsburgh, Pennsylvania 15213, USA*

¹¹*Enrico Fermi Institute, University of Chicago, Chicago, Illinois 60637, USA*

¹²*Comenius University, 842 48 Bratislava, Slovakia; Institute of Experimental Physics, 040 01 Kosice, Slovakia*

¹³*Joint Institute for Nuclear Research, RU-141980 Dubna, Russia*

¹⁴*Duke University, Durham, North Carolina 27708, USA*

¹⁵*Fermi National Accelerator Laboratory, Batavia, Illinois 60510, USA*

¹⁶*University of Florida, Gainesville, Florida 32611, USA*

¹⁷*Laboratori Nazionali di Frascati, Istituto Nazionale di Fisica Nucleare, I-00044 Frascati, Italy*

¹⁸*University of Geneva, CH-1211 Geneva 4, Switzerland*

¹⁹*Glasgow University, Glasgow G12 8QQ, United Kingdom*

²⁰*Harvard University, Cambridge, Massachusetts 02138, USA*

²¹*Division of High Energy Physics, Department of Physics, University of Helsinki,*

FIN-00014, Helsinki, Finland; Helsinki Institute of Physics, FIN-00014, Helsinki, Finland

²²*University of Illinois, Urbana, Illinois 61801, USA*

²³*The Johns Hopkins University, Baltimore, Maryland 21218, USA*

²⁴*Institut für Experimentelle Kernphysik, Karlsruhe Institute of Technology, D-76131 Karlsruhe, Germany*

²⁵*Center for High Energy Physics: Kyungpook National University,*

Daegu 702-701, Korea; Seoul National University, Seoul 151-742,

Korea; Sungkyunkwan University, Suwon 440-746,

Korea; Korea Institute of Science and Technology Information,

Daejeon 305-806, Korea; Chonnam National University,

Gwangju 500-757, Korea; Chonbuk National University, Jeonju 561-756,

Korea; Ewha Womans University, Seoul, 120-750, Korea

²⁶*Ernest Orlando Lawrence Berkeley National Laboratory, Berkeley, California 94720, USA*

²⁷*University of Liverpool, Liverpool L69 7ZE, United Kingdom*

²⁸*University College London, London WC1E 6BT, United Kingdom*

²⁹*Centro de Investigaciones Energeticas Medioambientales y Tecnologicas, E-28040 Madrid, Spain*

³⁰*Massachusetts Institute of Technology, Cambridge, Massachusetts 02139, USA*

³¹*University of Michigan, Ann Arbor, Michigan 48109, USA*

³²*Michigan State University, East Lansing, Michigan 48824, USA*

³³*Institution for Theoretical and Experimental Physics, ITEP, Moscow 117259, Russia*

³⁴*University of New Mexico, Albuquerque, New Mexico 87131, USA*

³⁵*The Ohio State University, Columbus, Ohio 43210, USA*

³⁶*Okayama University, Okayama 700-8530, Japan*

³⁷*Osaka City University, Osaka 558-8585, Japan*

³⁸*University of Oxford, Oxford OX1 3RH, United Kingdom*

³⁹*Istituto Nazionale di Fisica Nucleare, Sezione di Padova, ^{ll}University of Padova, I-35131 Padova, Italy*

⁴⁰*University of Pennsylvania, Philadelphia, Pennsylvania 19104, USA*

⁴¹*Istituto Nazionale di Fisica Nucleare Pisa, ^{mm}University of Pisa,*

ⁿⁿUniversity of Siena, ^{oo}Scuola Normale Superiore,

I-56127 Pisa, Italy, ^{pp}INFN Pavia, I-27100 Pavia,

Italy, ^{qq}University of Pavia, I-27100 Pavia, Italy

⁴²*University of Pittsburgh, Pittsburgh, Pennsylvania 15260, USA*

- ⁴³Purdue University, West Lafayette, Indiana 47907, USA
⁴⁴University of Rochester, Rochester, New York 14627, USA
⁴⁵The Rockefeller University, New York, New York 10065, USA
⁴⁶Istituto Nazionale di Fisica Nucleare, Sezione di Roma 1,
^{rr}Sapienza Università di Roma, I-00185 Roma, Italy
⁴⁷Mitchell Institute for Fundamental Physics and Astronomy,
Texas A&M University, College Station, Texas 77843, USA
⁴⁸Istituto Nazionale di Fisica Nucleare Trieste, ^{ss}Gruppo Collegato di Udine,
^{tt}University of Udine, I-33100 Udine, Italy, ^{uu}University of Trieste, I-34127 Trieste, Italy
⁴⁹University of Tsukuba, Tsukuba, Ibaraki 305, Japan
⁵⁰Tufts University, Medford, Massachusetts 02155, USA
⁵¹Waseda University, Tokyo 169, Japan
⁵²Wayne State University, Detroit, Michigan 48201, USA
⁵³University of Wisconsin-Madison, Madison, Wisconsin 53706, USA
⁵⁴Yale University, New Haven, Connecticut 06520, USA

A search for the exotic meson $X(5568)$ decaying into the $B_s^0 \pi^\pm$ final state is performed using data corresponding to 9.6 fb^{-1} from $p\bar{p}$ collisions at $\sqrt{s} = 1960 \text{ GeV}$ recorded by the Collider Detector at Fermilab. No evidence for this state is found and an upper limit of 6.7% at the 95% confidence level is set on the fraction of B_s^0 produced through the $X(5568) \rightarrow B_s^0 \pi^\pm$ process.

PACS numbers: 13.25Jx, 13.60.Le, 14.40.Rt

The new and unexpected structure in the $B_s^0 \pi^\pm$ final state recently observed by the D0 collaboration [1] in $p\bar{p}$ collisions at $\sqrt{s} = 1960 \text{ GeV}$ cannot be interpreted as a meson composed of a quark-antiquark pair. This reported signal, named $X(5568)$, is measured with a mass of $5567.8 \pm 2.9_{-1.9}^{+0.9} \text{ MeV}/c^2$ and a width of $21.9 \pm 6.4_{-2.5}^{+5.0} \text{ MeV}/c^2$. Several collaborations in both electron-positron and hadronic collision experiments have found evidence for other exotic hadron candidates formed with four or more quarks [2]. The $B_s^0 \pi^\pm$ final state contains four quark flavors, which cannot result from the decay of any standard meson. An observation of this state, if confirmed, would represent the first tetraquark (four-quark) candidate containing four different quark flavors. However, efforts by the LHCb and CMS collaborations to confirm the $X(5568)$ provide no supporting evidence for its existence [3, 4].

*Deceased

†With visitors from ^aUniversity of British Columbia, Vancouver, BC V6T 1Z1, Canada, ^bIstituto Nazionale di Fisica Nucleare, Sezione di Cagliari, 09042 Monserrato (Cagliari), Italy, ^cUniversity of California Irvine, Irvine, CA 92697, USA, ^dInstitute of Physics, Academy of Sciences of the Czech Republic, 182 21, Czech Republic, ^eCERN, CH-1211 Geneva, Switzerland, ^fCornell University, Ithaca, NY 14853, USA, ^gUniversity of Cyprus, Nicosia CY-1678, Cyprus, ^hOffice of Science, U.S. Department of Energy, Washington, DC 20585, USA, ⁱUniversity College Dublin, Dublin 4, Ireland, ^jETH, 8092 Zürich, Switzerland, ^kUniversity of Fukui, Fukui City, Fukui Prefecture, Japan 910-0017, ^lUniversidad Iberoamericana, Lomas de Santa Fe, México, C.P. 01219, Distrito Federal, ^mUniversity of Iowa, Iowa City, IA 52242, USA, ⁿKinki University, Higashi-Osaka City, Japan 577-8502, ^oKansas State University, Manhattan, KS 66506, USA, ^pBrookhaven National Laboratory, Upton, NY 11973, USA, ^qIstituto Nazionale di Fisica Nucleare, Sezione di Lecce, Via Arnesano, I-73100 Lecce, Italy, ^rQueen Mary, University of London, London, E1 4NS, United Kingdom, ^sUniversity of Melbourne, Victoria 3010, Australia, ^tMuons, Inc., Batavia, IL 60510, USA, ^uNagasaki Institute of Applied Science, Nagasaki 851-0193, Japan, ^vNational Research Nuclear University, Moscow 115409, Russia, ^wNorthwestern University, Evanston, IL 60208, USA, ^xUniversity of Notre Dame, Notre Dame, IN 46556, USA, ^yUniversidad de Oviedo, E-33007 Oviedo, Spain, ^zCNRS-IN2P3, Paris, F-75205 France, ^{aa}Universidad Tecnica Federico Santa Maria, 110v Valparaiso, Chile, ^{bb}Sejong University, Seoul 143-747, Korea, ^{cc}The University of Jordan, Amman 11942, Jordan, ^{dd}Université catholique de Louvain, 1348 Louvain-La-Neuve, Belgium, ^{ee}University of Zürich, 8006 Zürich, Switzerland, ^{ff}Massachusetts General Hospital, Boston, MA 02114 USA, ^{gg}Harvard Medical School, Boston, MA 02114 USA, ^{hh}Hampton University, Hampton, VA 23668, USA, ⁱⁱLos Alamos National Laboratory, Los Alamos, NM 87544, USA, ^{jj}Università degli Studi di Napoli Federico II, I-80138 Napoli, Italy

In this Letter we report the results of a search for the exotic meson $X(5568)$. This search is made in $p\bar{p}$ collisions at a center of mass energy of 1.96 TeV using the Collider Detector at Fermilab (CDF II) by reconstructing the decay chain $X(5568) \rightarrow B_s^0 \pi^\pm$, $B_s^0 \rightarrow J/\psi \phi$, $J/\psi \rightarrow \mu^+ \mu^-$, and $\phi \rightarrow K^+ K^-$. These studies use the full CDF II data sample corresponding to an integrated luminosity of 9.6 fb^{-1} and constitute the first search for $X(5568)$ production in the same initial conditions as the D0 observation.

The CDF II detector is described in detail elsewhere [5]. This analysis uses the tracking and muon identification systems. The tracking system measured the trajectories of charged particles (tracks) and consisted of five layers of double-sided silicon detectors [6] and a 96 layer open-cell drift chamber (COT) [7] that operated inside a solenoid with a 1.4 T field oriented along the beam direction. Charged particles with transverse momentum (p_T) greater than 250 MeV/ c that originated from the collision point were measured in the tracking system with a transverse-momentum resolution of $\sigma(p_T)/p_T^2 \approx 0.0008 (\text{GeV}/c)^{-1}$. Muon candidates from the decay $J/\psi \rightarrow \mu^+ \mu^-$ were identified by two sets of drift chambers located radially outside electromagnetic and hadronic calorimeters [8]. The central muon chambers covered the pseudorapidity region $|\eta| < 0.6$ and were sensitive to muons with $p_T > 1.4 \text{ GeV}/c$. A second muon system covered the region $0.6 < |\eta| < 1.0$ and detected muons having $p_T > 2.0 \text{ GeV}/c$.

The mass resolution and acceptance for the $X(5568)$ and B_s^0 decays are studied with a Monte Carlo simulation that generates $X(5568) \rightarrow B_s^0 \pi^\pm$ decays consistent with CDF measurements of p_T and rapidity distributions for inclusive B_s^0 production. The simulated $X(5568)$ and B_s^0 decay isotropically and other final-state decay processes are simulated with the EVTGEN [9] program. The generated events are passed through the detector and trigger simulation based on a GEANT3 description [10] and processed through the same reconstruction and analysis algorithms used for the data.

This analysis is based on events recorded with a three-level trigger that was dedicated to the collection of a $J/\psi \rightarrow \mu^+ \mu^-$ sample. The first level of the trigger system required two muon candidates with tracks in the COT and muon chamber systems that matched in the plane transverse to the beam direction. At this stage, the trigger system identified trigger tracks with $p_T > 1.4 \text{ GeV}/c$ and segmented into 1.25° in the azimuthal angle. The second level imposed the requirement that the muon candidates have opposite charge and limited the accepted range of opening angle between them [11]. The third level of the trigger reconstructed the muon pair with the full resolution of the

COT, and required that the invariant mass of the pair fall within the range 2.7–4.0 GeV/ c^2 .

The strategy for this analysis is to reconstruct the $B_s^0 \pi^\pm$ final state using similar methods to those used by previous CDF analyses [11, 12]. The measured yields and acceptances are used to calculate the fraction of B_s^0 produced through the process $X(5568) \rightarrow B_s^0 \pi^\pm$, given by

$$f_{B_s^0/X(5568)} = \frac{\sigma(p\bar{p} \rightarrow X(5568) + x) \times \mathcal{B}(X(5568) \rightarrow B_s^0 \pi^\pm)}{\sigma(p\bar{p} \rightarrow B_s^0 + x)} = \frac{N_X}{N_{B_s^0}} \frac{1}{\alpha_{X,B_s^0}}, \quad (1)$$

where N_X and $N_{B_s^0}$ are the numbers of $X(5568)$ and B_s^0 reconstructed in the data, respectively, and α_{X,B_s^0} is the acceptance and reconstruction efficiency for the $X(5568)$ in events where the B_s^0 is reconstructed. In the absence of an $X(5568)$ signal, this expression is used to calculate a limit on $f_{B_s^0/X(5568)}$.

The analysis of the data begins with a selection of well-measured $J/\psi \rightarrow \mu^+ \mu^-$ candidates. The trigger requirements are confirmed by selecting events that contain two oppositely charged muon candidates, each with matching COT and muon chamber tracks. Both muon tracks are required to have associated measurements in at least three layers of the silicon detector, and are fit with the constraint that they originate from a common decay point. Dimuon candidates are measured with an average mass resolution of 20 MeV/ c^2 and candidates with a mass within 80 MeV/ c^2 of the world-average J/ψ mass [13] are retained as J/ψ candidates. Approximately 15 million J/ψ candidates are obtained.

The reconstruction of ϕ candidates uses all additional tracks found in each event containing a J/ψ candidate. Pairs of oppositely charged tracks with three or more silicon layer measurements and $p_T > 400$ MeV/ c are assigned the K^\pm mass and have their track parameters recalculated according to a fit that constrains them to intersect. Candidates whose fits converge have a mass measurement resolution that is insignificant compared to the ϕ natural width of 4.2 MeV/ c^2 [13], and those with an invariant mass within 10 MeV/ c^2 of the world-average ϕ mass [13] are retained as ϕ candidates.

The sample of B_s^0 candidates is obtained by selecting all candidates where the four tracks satisfy a fit that constrains the tracks to originate from a common decay point and the dimuon to have the world-average J/ψ mass [13]. Further requirements placed on the B_s^0 candidates include $p_T > 10$ GeV/ c and $ct > 100$ μm , where t is the proper decay time of the candidate. These requirements remove candidates for which the acceptance of the detector is low and reduce background due to prompt combinations. The $J/\psi \phi$ mass distribution obtained is shown in Fig. 1. The number of

B_s^0 candidates in the data is obtained by performing a binned likelihood fit on the distribution in Fig. 1 with a linear background model and two Gaussian functions with a common central value as a signal model. We measure a B_s^0 yield of $N_{B_s^0} = 3552 \pm 65$ candidates and a mass of $5366.5 \pm 0.2 \text{ MeV}/c^2$, consistent with the world average [13]. The average mass measurement resolution is $11 \text{ MeV}/c^2$ and candidates with mass within $30 \text{ MeV}/c^2$ of the nominal B_s^0 mass are used for the $X(5568)$ search. Mass sidebands are also indicated in Fig. 1 and are defined as two mass ranges of $30 \text{ MeV}/c^2$ full width centered $\pm 100 \text{ MeV}/c^2$ from the nominal B_s^0 mass.

The final $B_s^0 \pi^\pm$ sample is obtained by combining the B_s^0 candidate tracks with the remaining tracks, assumed to be pions, that have three or more silicon detector hits and $p_T > 400 \text{ MeV}/c$. A constrained fit is performed and requires the B_s^0 and π^\pm candidates to originate from the same point. This final selection also requires the transverse displacement of the full final state with respect to the beamline to be less than $100 \mu\text{m}$. A mass resolution of $1.8 \text{ MeV}/c^2$ is obtained for the $B_s^0 \pi^\pm$ final state by defining $M(B_s^0 \pi^\pm) = M(J/\psi \phi \pi^\pm) - M(J/\psi \phi) + M_{B_s^0}$, where $M_{B_s^0}$ is the world-average value of the mass of the B_s^0 [13].

Simulated events are used to estimate the acceptance of the B_s^0 and the relative acceptance α_{X, B_s^0} for the $X(5568)$ for events containing a reconstructed B_s^0 . A correction is made to the generated $X(5568)$ sample so that the simulated $p_T(B_s^0)$ distribution is identical to the acceptance-corrected $p_T(B_s^0)$ distribution observed in the data. Three simulated samples are generated using widths of the $X(5568)$, with values of 21.6, 15.5, and $28.7 \text{ MeV}/c^2$. These correspond to the central value and the range of the uncertainty for the width measured in the reported $X(5568)$ [1].

The shape of the $B_s^0 \pi^\pm$ mass distributions obtained from simulated events is dependent on p_T , due to the acceptance and efficiency of the tracking system. The reconstructed signal shape expected for the $X(5568)$ is obtained by integrating the p_T -dependent mass distribution shapes found in simulation with a weighting determined by the observed $p_T(B_s^0)$ distribution. The expected mass-distribution shape is parametrized with an empirical function using two Gaussians and a tail term on the high-mass side from the peak. The yield of $X(5568)$ observed in the simulated events provides a value of $\alpha_{X, B_s^0} = 0.445 \pm 0.027$ for $p_T(B_s^0) > 10 \text{ GeV}/c$, where the uncertainty is statistical. A systematic variation on α_{X, B_s^0} of ± 0.018 is found due to the uncertainty on the reported width of the $X(5568)$.

The $B_s^0 \pi^\pm$ mass distribution is analyzed with an unbinned likelihood fit with the likelihood calculated as

$$\mathcal{L} = \prod_i^N [f\mathcal{S}(m_i) + (1-f)\mathcal{B}(m_i)], \quad (2)$$

where N is the number of entries in the distribution, m_i is the mass of entry i , f is the signal fraction obtained from the fit, $\mathcal{S}(m_i)$ is the signal model obtained from simulation and $\mathcal{B}(m_i)$ is the background model. The functional form of $\mathcal{B}(m_i)$ is obtained by fitting the mass distribution with all candidates within the central value of the reported width ($21.6 \text{ MeV}/c^2$) [1] of the $X(5568)$ mass value omitted, with f fixed at the value that results from the D0 observation, and $\mathcal{B}(m_i)$ modeled with a polynomial. Variations in this fit are also made, corresponding to the uncertainty on the signal yield in the D0 measurement. The background model is shown overlaid on the data in Fig. 2.

The background model obtained in this process is fixed in the fit of the full set of candidates where f is allowed to float. This fit is overlaid on the data in Fig. 3 and estimates an $X(5568)$ yield of $N_X = 36 \pm 30$ candidates. The signal and background models were varied by the uncertainties in the D0 measurements on the mass, width, and production rate of the $X(5568)$ to provide a systematic uncertainty estimate of 14 candidates. This signal yield is used in Eq. (1) with the acceptance and B_s^0 yield to calculate $f_{B_s^0/X(5568)} = (2.3 \pm 1.9(\text{stat}) \pm 0.9(\text{syst}))\%$. Fig. 3 also shows the $M(B_s^0 \pi^\pm)$ distribution obtained from the $J/\psi\phi$ candidates in the B_s^0 mass sidebands indicated in Fig. 1 for comparison.

The $X(5568)$ yield obtained in the data is consistent with no signal. Therefore, the fit where the signal is allowed to float is compared to the null hypothesis by repeating the fit where the signal component is omitted. The value of twice the difference in the logarithm of the likelihood, $2\delta \log \mathcal{L}$, between the fits is then used as a measure of the compatibility of the data with the background-only hypothesis. An upper limit on the presence of an $X(5568)$ signal is calculated by following a frequentist Neyman construction. The technique uses simulated mass distributions with a shape given by the probability distribution in Eq. (2). Various signal-strength hypotheses are generated by fixing $f_{B_s^0/X(5568)}$ for each simulation, producing a signal fraction given by $f = N_X/N$. Ten thousand trials are run for each signal-strength hypothesis and the mass distributions obtained in each trial are fit twice as in the data, once with a floating signal fraction and once with the null signal hypothesis. The $2\delta \log \mathcal{L}$ is then evaluated for all simulated distributions.

The results of these simulations are used to set an upper limit on $f_{B_s^0/X(5568)}$. The cumulative probability distribution of $2\delta \log \mathcal{L}$ for a given $f_{B_s^0/X(5568)}$ provides the test statistic. The 95% confidence level, C.L., upper limit is obtained by determining the value of $f_{B_s^0/X(5568)}$ where the value of the cumulative probability distribution, evaluated at the value of $2\delta \log \mathcal{L}$ seen in the data, approximates 0.05. A value of $f_{B_s^0/X(5568)} = 0.055$ is obtained by this method.

Alternative background models that use a $B^0 \rightarrow J/\psi K^*(892)^0$ sample have also been used to obtain upper limits on $f_{B_s^0/X(5568)}$ through this technique. The alternative models are found by fitting the $B^0\pi^-$ and $B^0\pi^+$ mass distributions and omitting mass regions corresponding to the $B_1(5721)^+$ or $B_2^*(5747)^+$ (for $B^0\pi^+$). These background models are then used to repeat the simulations used in the calculations for the upper limit. These alternatives give upper limits on $f_{B_s^0/X(5568)}$ that are comparable to the result based on the $B_s^0\pi^\pm$ fit.

Two systematic effects are considered that modify the upper limit obtained for $f_{B_s^0/X(5568)}$. The first takes into account uncertainties on the quantities in Eq. (1). The uncertainties on the quantities are combined in quadrature to obtain an overall relative uncertainty of 6.6%, where the uncertainty on the acceptance (α_{X,B_s^0}) provides the largest contribution (6.0%). The second systematic uncertainty is due to the background model. An alternative model, where the input value of $f_{B_s^0/X(5568)}$ is increased by one standard deviation with respect to the D0 central value tests this sensitivity. An upper limit of $f_{B_s^0/X(5568)} = 0.060$ is found for this background model, so a relative uncertainty of 9% is assigned to this effect. Combining these in quadrature gives a total systematic uncertainty of 11% on this measurement of $f_{B_s^0/X(5568)}$. We treat the systematic uncertainty as a normal distribution width, and consider twice its value to correspond to a 95% fluctuation. Consequently, inclusion of the systematic uncertainty provides a 95% C.L. upper limit on $f_{B_s^0/X(5568)}$ of 0.067.

In conclusion, a search for the exotic meson $X(5568)$ is performed with the full CDF II data set, which was obtained with the same collision conditions and similar kinematic range as in the original observation of this state by D0 [1]. No statistically significant evidence for the process $X(5568) \rightarrow B_s^0\pi^\pm$ is found. A 95% C.L. upper limit of 6.7% is found for fraction of B_s^0 produced through this process. Consequently, this analysis does not confirm the existence of the $X(5568)$.

This document was prepared by the CDF collaboration using the resources of the Fermi National Accelerator Laboratory (Fermilab), a U.S. Department of Energy, Office of Science, HEP User Facility. Fermilab is managed by

Fermi Research Alliance, LLC (FRA), acting under Contract No. DE-AC02-07CH11359. We thank the Fermilab staff and the technical staffs of the participating institutions for their vital contributions. This work was supported by the U.S. Department of Energy and National Science Foundation; the Italian Istituto Nazionale di Fisica Nucleare; the Ministry of Education, Culture, Sports, Science and Technology of Japan; the Natural Sciences and Engineering Research Council of Canada; the National Science Council of the Republic of China; the Swiss National Science Foundation; the A.P. Sloan Foundation; the Bundesministerium für Bildung und Forschung, Germany; the Korean World Class University Program, the National Research Foundation of Korea; the Science and Technology Facilities Council and the Royal Society, United Kingdom; the Russian Foundation for Basic Research; the Ministerio de Ciencia e Innovación, and Programa Consolider-Ingenio 2010, Spain; the Slovak R&D Agency; the Academy of Finland; the Australian Research Council (ARC); and the EU community Marie Curie Fellowship Contract No. 302103.

-
- [1] V.M. Abazov *et al.* (D0 Collaboration), *Phys. Rev Lett.* **117**, 022003 (2016).
 - [2] S.L. Olsen, *Front. Phys.* **10**, 101401 (2016).
 - [3] R. Aaij *et al.* (LHCb Collaboration), *Phys. Rev Lett.* **117**, 152003 (2016).
 - [4] CMS Collaboration, arXiv:1712.06144v1 (2017).
 - [5] D. Acosta *et al.* (CDF Collaboration), *Phys. Rev. D* **71**, 032001 (2005); T. Affolder *et al.*, *Nucl. Instrum. Methods, Sec. A* **526**, 249 (2004).
 - [6] T. Aaltonen *et al.*, *Nucl. Instrum. Methods, Sec. A* **729**, 153 (2013).
 - [7] T. Affolder *et al.*, *Nucl. Instrum. Methods, Sec. A* **526**, 249 (2004).
 - [8] G. Ascoli *et al.*, *Nucl. Instrum. Methods, Sec. A* **268**, 33 (1988).
 - [9] D.J. Lange, *Nucl. Instrum. Methods Phys. Res., Sect. A* **462**, 152 (2001).
 - [10] R. Brun, R. Hagelberg, M. Hansroul, and J.C. Lassalle, CERN Reports No. CERN-DD-78-2-REV and No. CERN-DD-78-2.
 - [11] A. Abulencia *et al.* (CDF Collaboration), *Phys. Rev D* **75**, 012010 (2007).
 - [12] T. Aaltonen *et al.* (CDF Collaboration), *Phys. Rev D* **89**, 072014 (2014).
 - [13] C. Patrignani *et al.* (Particle Data Group), *Chinese Physics C*, **40**, 100001 (2016).

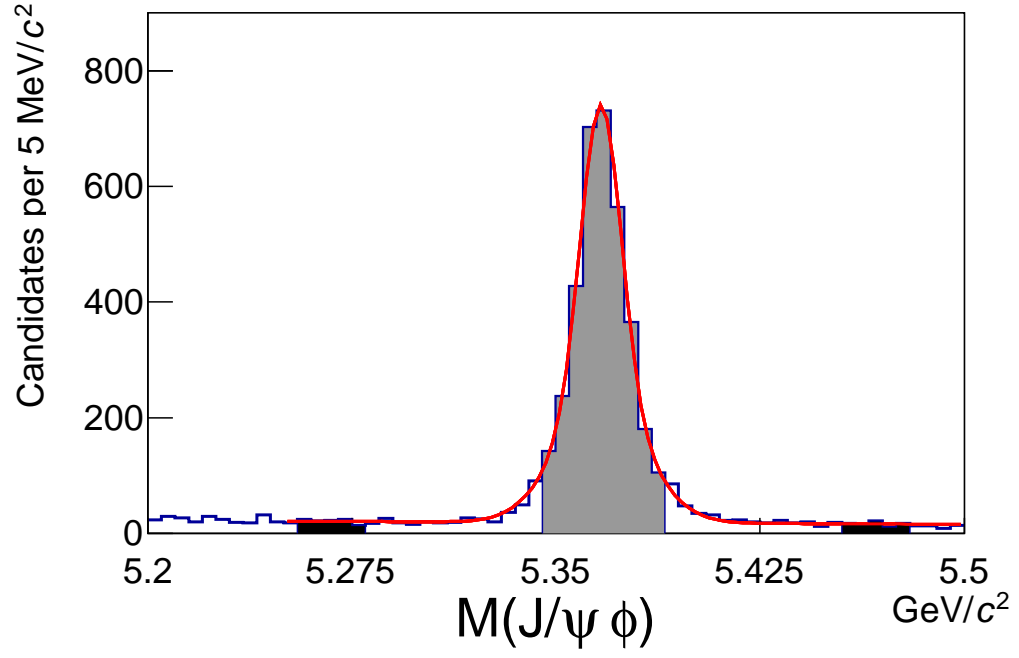


FIG. 1: Distribution of $J/\psi \phi$ mass for $p_T > 10 \text{ GeV}/c$ with the fit overlaid on the histogram. The B_s^0 signal region is highlighted in gray. Areas used to define backgrounds based on the mass sidebands are indicated in black.

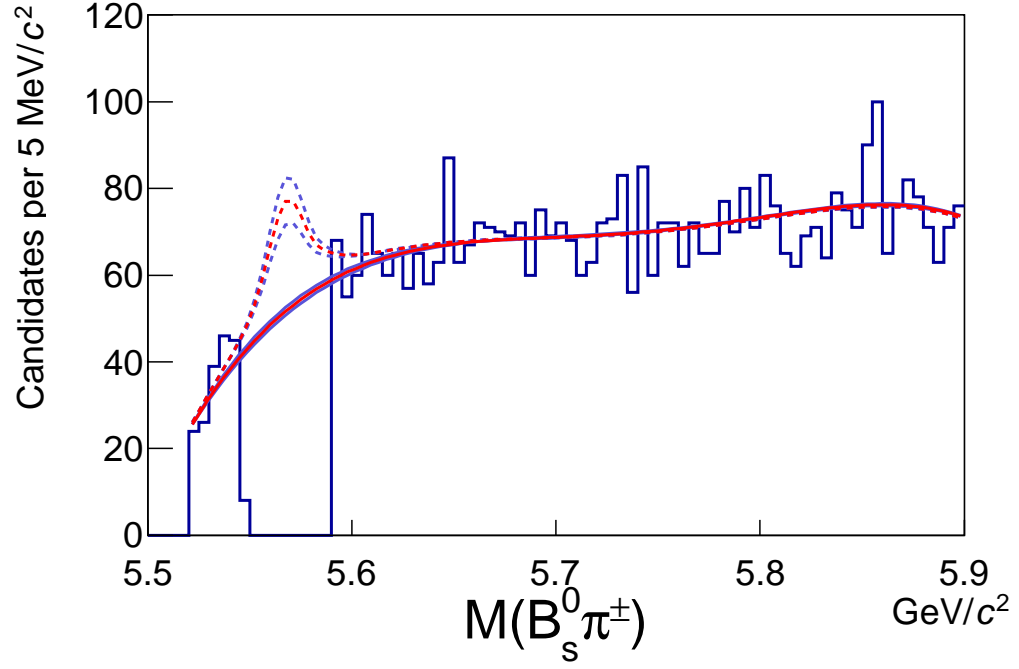


FIG. 2: Distribution of $B_s^0 \pi^\pm$ mass where the candidates within $21.6 \text{ MeV}/c^2$ of the $X(5568)$ are omitted. The background model is overlaid in a solid line, where the line width indicates $\pm\sigma$ variations on the background model due to variations in the assumption for the $X(5568)$ signal amplitude. Dashed curves indicate the signal components used to obtain the background model and its variations.

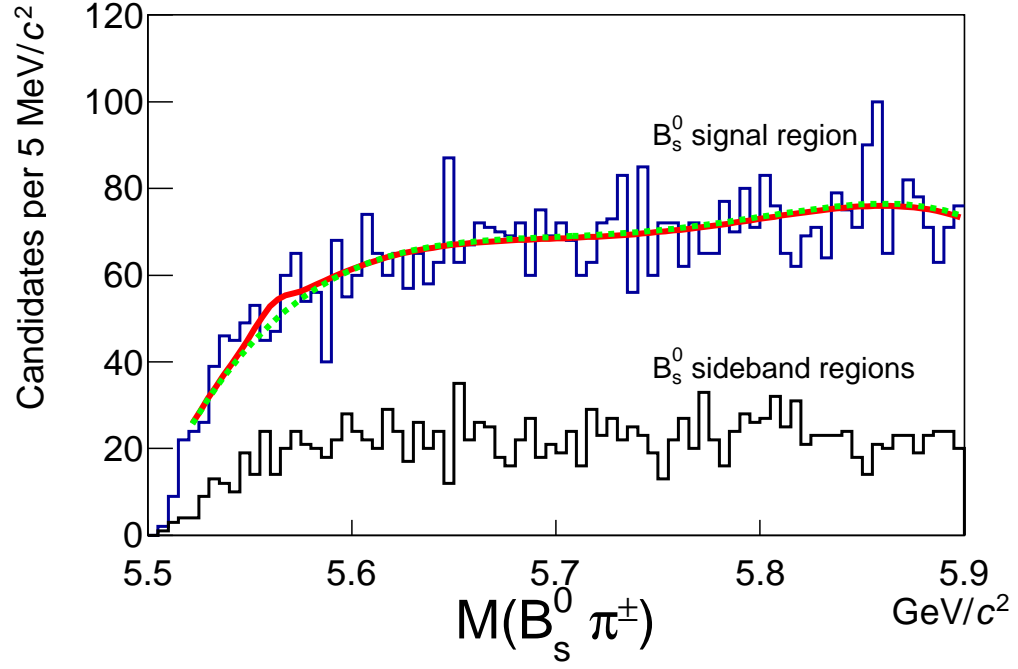


FIG. 3: Distribution of $B_s^0 \pi^\pm$ mass for $p_T(B_s^0) > 10 \text{ GeV}/c$, for candidates in the B_s^0 mass range and for the mass sidebands, as indicated. The fit to the data with a freely floating (null) signal is overlaid in a solid (dashed) line.